Int. J. Solids Structures, 1969, Vol. 5, pp. 303 to 317. Pergamon Press. Printed in Great Britain

PROPAGATION OF LARGE AMPLITUDE WAVES IN ANNEALED BRASS

WILLIAM F. HARTMAN*

The Johns Hopkins University, Baltimore, Maryland

Abstract—An experimental investigation of large amplitude wave propagation in annealed α-brass polycrystals demonstrates the applicability of the generalized parabolic stress–strain relationship to a binary alloy of low stacking-fault energy. Several discrete deformation modes are found to be operative depending on the material history prior to free-flight impact of rods. The results are found to be in agreement with quasi-static deformation of brass single crystals and polycrystals. It is concluded that, in spite of the large difference in the stacking-fault energies of brass and aluminum, the deformations of each can be precisely described without explicitly including "strain rate" into the constitutive equation of either.

INTRODUCTION

THE development of appropriate constitutive equations which describe the dynamic response of metals has often been the objective of experimental research in solid mechanics. The theme of many investigations concerns the problem of whether or not the variable "strain rate" should be included in the argument of the stress response function. A motivation that it should is provided by the researches in dislocation mechanisms. On the other hand, precise and accurate description of the dynamic behavior of metals from a continuum point of view has been consistently obtained by Bell [1] in terms of a generalized constitutive relationship which does not explicitly contain the rate of strain as a relevant parameter. The work of many experimentalists, including Bell, has provided extensive data for the propagation of plastic waves in the face-centered cubic metal aluminum. The degree to which "viscosity" is considered important by these authors is as various as the experimental techniques employed by them. This author considers the technique of Bell to be the best direct measurement of the large amplitude plastic wave. Accordingly, employing this technique to study large amplitude wave propagation in a face-centered cubic solid which has a dislocation property appreciably distinct from aluminum would facilitate establishing the extent of Bell's generalization. A typical structural parameter, the stacking-fault energy, is very high for aluminum. A face-centered cubic alloy which has a very low stacking-fault energy is α-brass. Therefore this paper presents experimental data on the propagation of plastic waves in annealed polycrystalline brass rods.

Large uniaxial deformations of many metallic single crystals and polycrystals may be described in terms of a generalized parabolic stress–strain relationship, whose coefficient is always one of a set of discrete values which are related to the material's zero point isotropic elastic shear modulus [1]. These discrete values define deformation modes which can be correlated with the purity and thermo-mechanical history of the metal. During quasistatic plastic deformations, the work-hardening may be characterized by several of

* Presently at the University of Minnesota, Minneapolis, Minnesota.

these modes, each operative for a certain deformation region whose extremities define transitional strains. Many examples of these transitional deformations are given in [1], where it is also shown that one deformation mode remains stable during impact deformations. Furthermore, it is typical in the aluminum impact experiments of Bell that the same deformation mode is always operative. It will be shown in this paper that because of variations in pre-impact histories several deformation modes are found to govern the dynamic response of annealed polycrystalline brass rods during free flight impact. The results will be correlated with quasistatic deformations of brass polycrystals and single crystals [2].

The generalized stress–strain relationship, whose applicability to the dynamic deformation of brass is herein examined, can be written as:

$$\sigma = \beta_r(0)(1 - T/T_m)\varepsilon^{\frac{1}{2}} \tag{1}$$

where the zero point parabola coefficient is given as

$$\beta_r(0) = (\tfrac{2}{3})^{r/2}\mu(0)B_0 \tag{2}$$

The uniaxial stress σ is referred to the initial configuration and is often called "nominal stress"; ε is the absolute value of the finite deformation measure $\partial u/\partial X$, "nominal strain", where X is the material coordinate in the axial direction and $u = x - X$ is the displacement; r is a non-negative integer and is called the deformation mode index; B_0 is a dimensionless constant, 0·0280; T is the temperature in degrees Kelvin; T_m is the melting temperature, and $\mu(0)$ is the shear modulus at absolute zero.

EXPERIMENTAL PROCEDURE

Annealed specimens of solid brass circular cylinders, 2·51 cm in diameter and ranging from 17 to 45 cm in length, were subjected to unconstrained constant velocity axial compressive impact by annealed or hard brass cylinders, which were projected from an air gun. For each test the resulting longitudinal strain history on the surface at a material location between one and three diametrical lengths from the impact face was recorded by a diffraction grating strain gage ruled on the polished rod. The details of this technique are identical with those described by Bell [3]. The gage length of the grating was 0·127 mm, corresponding to 154 ruled lines. After impact the diameters of the hitter and specimen were measured with a pair of micrometer calipers to determine the residual radial strain distribution.

The copper, zinc, lead and iron percentages of the rods were 70·15, 29·71, 0·01, 0·02, respectively. The density of this material is 8·55 g/cm^3. The melting temperature shall always be considered as the solidus temperature, 1188°K. The zero point shear modulus is 4600 kg/mm^2. The specimens were obtained from 1 in. dia. cold drawn (30 per cent reduction of area) rods, annealed at 755°K for 2 hr, furnace cooled, carefully machined to a dia. of 2·51 cm, and polished with fine rouge on a buffing wheel. The tests were conducted at room temperature.

The specimens were annealed to reduce any anisotropies resulting from fabrication and to promote as little micromorphology as was still compatible with the intent to investigate polycrystalline aggregates. The particular annealing process was selected because of the resulting favorable grain size and yield stress, which were about 0·03 mm and 10·5 kg/mm^2.

This grain size ensures that the area of the grating, from which the monitored diffracted light emanates, contains at least thirty grains. Therefore, even though a small gate length is employed, a sufficiently large granular sample guarantees the measurement of a truly "aggregate" strain. The yield stress, although large compared to fully annealed metals, is small enough so as to provide plastic deformation at low impact speeds.

The thermomechanical histories of all specimens prior to their reported impacts were not identical. There existed small variations in the annealing environment and cooling characteristics. In some of the tests the specimens had been previously impacted at velocities less than the yield velocity. Although these mild variations were initially assumed to be insignificant, it was later concluded that they appreciably influenced the deformation behavior. The details of this dependence will evolve in the analysis of the data.

The strain vs. time and surface angle vs. time data for each of the twenty-five tests are given in [2].

DATA ANALYSIS AND DISCUSSION

Discrete deformation modes

The finite amplitude wave theory of von Karman [4] and Taylor [5] predicts that the wave speed, $C_p(\varepsilon_0)$, for each value of strain, ε_0, shall be constant and that the longitudinal particle velocity $\dot{u}(X, t)$, associated with $\varepsilon(X, t)$ is obtained in terms of $C_p(\varepsilon)$. These relations are represented by equations (3) and (4).

$$C_p(\varepsilon) = \left[\frac{d\sigma}{d\varepsilon}\frac{1}{\rho_0}\right]^{\frac{1}{2}} = \frac{X}{t}, \tag{3}$$

where ρ_0 is the mass density in the initial configuration;

$$\dot{u} = \int_0^{\varepsilon} C_p(\varepsilon')\, d\varepsilon'. \tag{4}$$

If through experiment these relations are found to hold, then the theory is known to apply and integration of equation (4) provides the determination of the stress–strain relationship. This technique is not employed here; rather the form of the stress–strain relationship will be assumed. However, verification of constant wave speeds and the prediction of maximum strains from equation (4) shall be obtained for certain values of r from equation (2).

Assuming the stress–strain relation to be of the form:

$$\sigma = \beta\varepsilon^a, \tag{5}$$

the technique described by Filbey [6] then results in the determination of a. Substitution of equation (5) into equation (3) and taking the logarithm of both sides yields

$$\frac{\Delta \log \varepsilon}{\Delta \log(X/t)} = \frac{2}{a-1}. \tag{6}$$

Examples of this determination of a a are shown in Fig. 1.

The use of equation (6) presumes that each level of strain propagates directly from the impact face with its own constant wave speed according to the constitutive relation of

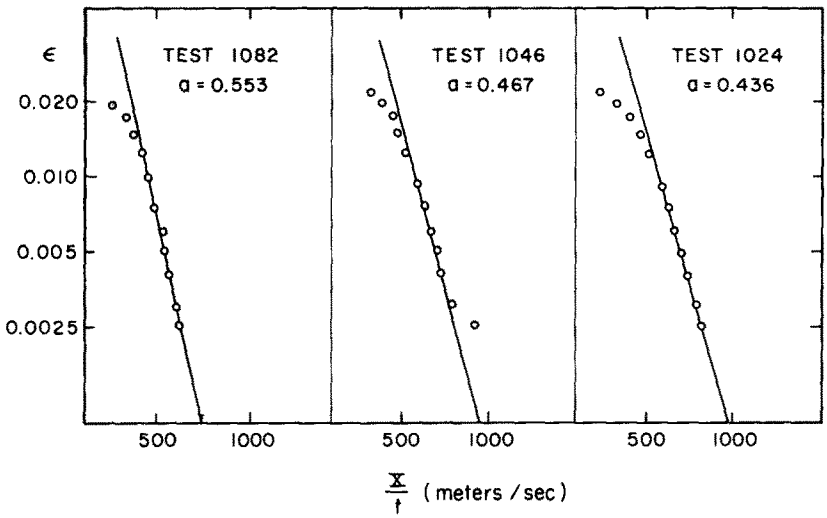

FIG. 1. Examples of log–log determination of the power exponent a.

equation (5). Bell [1] has shown for several metals that such an assumption, with $a = \frac{1}{2}$, is valid for strains below a certain value, which arrives at the time of the surface angle maximum. The strains above this are delayed near the impact face in proportion to the amplitude of the wave, but having left the first diameter they propagate with their respective constant wave speeds; i.e. the propagation of the entire wave between stations outside the first diameter is governed by equation (5). Furthermore, within the first diameter, one dimensional observations are in variance with those consistent measurements of longitudinal strain downstream. The complexities of the first diameter are generated by large elastic dilatational wave fronts, which prior to reaching one diametrical length become sufficiently extinguished through self-interaction so that proper observation of the one dimensional finite amplitude plastic wave is possible. Therefore, observations outside the first diameter are preferred unless the mechanics of that region is the topic of study.

Since a mild nonaxiality can extend the first diameter complication, measurements performed near one diametrical length can be anomalous. Of the 25 impact tests, the diffraction grating was located just inside one diameter in one test (1028) and just beyond it in three tests (1026, 1172, 1201). Table 1 indicates that all but one of these tests gave very low values of a as compared with the overall average of 0·420 for all tests. Nevertheless,

TABLE 1. THE VALUE OF a IS THAT DETERMINED FROM A LOG–LOG PLOT SUCH AS IN FIG. 1

Test number	Specimen length (cm)	Grating position (cm)	Hitter speed (cm/sec)	a
1015	25·25	4·82	3510	0·600
1018	17·80	3·78	3462	0·504
1019	17·80	3·68	3400	0·485
1020	25·40	3·68	2860	0·511
1024	25·40	3·18	2825	0·436
1026	25·40	2·64	2880	0·250

TABLE 1—*continued*

Test number	Specimen length (cm)	Grating position (cm)	Hitter speed (cm/sec)	a
1028	25·40	2·32	2870	0·156
1046	30·50	5·08	2700	0·467
1079	30·50	5.00	3000	0·425
1082	30·50	4·95	2970	0·553
1090	30·50	5·20	2820	0·400
1100	35·55	7·66	2740	0·490
1109	7·62	4.95	2900	0·439
1133	43·20	7·62	2420	0·523
1145	43·20	7·64	2420	0·660
1170	43·20	7.70	3150	0·545
1172	25·40	2·59	2420	0·475
1197	30·50	3·81	2440	0·292
1198	30·50	3·87	2360	0·280
1199	30·50	3·92	2430	0·362
1201	25·00	2·58	2340	0·290
1205	30·50	4·67	1985	0·356
1206	30·50	3·88	1800	0·420
1208	25·40	3·23	1460	0·165
1234	30·50	5·10	2600	0·432

this value suggests a reasonable description when the stress–strain law of each test is considered parabolic. The significance of this choice can be judged by the results it yields.

For a parabola, solving equation (3) for β yields

$$\beta = 2\rho_0(X/t)^2\varepsilon^{\frac{1}{2}}. \tag{7}$$

By calculating β from equation (7) for various values of ε over a strain–time curve, an average parabola coefficient may be obtained for that test. Bell and Werner [7] obtained parabola coefficients for copper by this process. For brass this calculation was performed at the strain values indicated in Table 2. For sixteen tests, which had power exponents

TABLE 2. THE PARABOLA COEFFICIENTS, $\beta(\varepsilon)$, FOR EACH TEST ARE THE VALUES CALCULATED FROM EQUATION (7) DIVIDED BY $(1-T/T_m)$. THEREFORE, β_{avg} REPRESENTS A MEAN PARABOLA COEFFICIENT AT 0°K OBTAINED FROM IMPACT DATA AT 300°K

Test No.	$\beta(\varepsilon)$ $\varepsilon = 0{\cdot}0030$	0·0050	0·0075	0·0100	0·0125	0·0150	0·0175	0·0200	0·0225	0·0250	β_{avg}
1015	54·2	54·6	57·6	60·1	57·8	57·4					57·0
1018	91·1	84·6	85·9	86·6	85·3	83·3	81·9	77·2			84·5
1019	88·8	83·3	83·6	84·4	83·8	80·8	79·5	73·2			82·2
1020	59·8	58·5	58·5	53·7							57·6
1024	76·3	73·5	71·5	69·8							72·8
1026	92·2	69·4	58·4	50·5							67·6
1028	87·4	72·0	61·3	54·8							68·9
1046	79·3	74·8	73·2	70·1	67·1	63·4					71·3
1079	58·2	56·4	56·4	54·7	53·4						55·8
1082	43·6	48·2	47·0	47·0	46·2						46·4
1090	114·1	98·8	93·5	93·5	91·2	85·4	82·5	80·0	77·2		90·7
1100	51·4	50·8	50·5	49·7	47·2						49·9

TABLE 2—*continued*

Test No.	$\beta(\varepsilon)$ $\varepsilon = 0{\cdot}0030$	0·0050	0·0075	0·0100	0·0125	0·0150	0·0175	0·0200	0·0225	0·0250	β_{avg}
1109	85·7	78·2	74·1	71·1	71·3	67·5	65·1				73·7
1133	45·0	43·6	45·5	45·3	44·9						44·9
1145	40·5	41·6	46·9	48·1	47·6						44·9
1170	44·4	52·6	56·2	60·5	61·3	63·0	63·1	62·7	61·5	60·4	58·6
1172	112·2	84·2	86·5	84·2	85·6	82·3	78·6	75·8			86·2
1197	67·3	62·0	53·7	49·7							58·2
1198	93·5	75·3	68·3	63·6	60·9	54·8					69·4
1199	111·8	83·2	90·4	88·6	89·8	84·2	84·2	82·7	78·6	73·5	86·7
1205	77·2	72·7	70·1	67·2	64·2	59·4					68·5
1206	76·5	73·3	73·3	67·9	66·0	61·3	58·0				68·0
1208	72·0	56·5	55·4	49·6							58·4
1234	44·8	44·6	43·0	40·8	39·8						42·6

within 20 per cent of $\frac{1}{2}$ and an average value of 0·494, the contribution to the average β was terminated when the data departed from the straight line of the log–log plot. This departure usually occurred following the strain corresponding to the arrival of the surface angle maximum, which is compatible with the observations by Bell [8] of the first diameter delay in the development of the upper levels of strain. Therefore, for the remaining nine tests, whose log–log determined power exponents differed from $\frac{1}{2}$ by more than 20 per cent, entries in Table 2 were made for those values up to the strain corresponding to the surface angle maximum. Each entry in Table 2 has been divided by $(1 - T/T_m)$ so as to yield parabola coefficients at zero degrees Kelvin, assuming Bell's temperature dependence. The averaged coefficients obtained by this process range from 42·6 to 124·1 kg/mm^2; however, there exist four definite intervals into which all but one value fall. These are seen in Fig. 2 wherein the average of each group is seen to correspond to a value of $\beta_r(0°)$ from equation (2) for four values of r. The agreement is extremely good; the maximum percentage difference of $\bar{\beta}_{avg}$ from $\beta_r(0°)$ being 2·1 per cent for $r = 5$. Moreover, the average deviation from the predicted values for all groups is 3·1 per cent. Test 1201 is not represented in Fig. 2; however, it corresponds to the value for $r = 0$.

This resulting agreement with predicted allowable coefficients suggests in itself appreciable merit for the parabolic assumption. However, as can be noticed from Table 2, this parabolic fit to the propagation data is not close for several tests. In fact, six tests, whose log–log determined power exponents are 20 per cent different from $\frac{1}{2}$, have a mean average deviation from their calculated parabola coefficients of 13·8 per cent in contrast to 4·9 per cent for all the others. That the average power exponent for these tests is 0·240 could have significance with respect to a $\frac{1}{4}$ power law as observed by Gillich [9] in aluminum single crystals. However, Gillich was unable to properly measure maximum strains; while here the maximum strains agree very well with the parabola coefficients fitted to the wave speed data. Hence it is appropriate to examine all the data of all the tests with respect to equation (1).

The representation of the impact test by four values of r implies a highly sensitive material with respect to the establishment or persistence of a deformation mode. The existence of four groups was noticed after fifteen tests had been conducted and immediately suggested a closer scrutiny of material history. It was found that discrepancies existed in

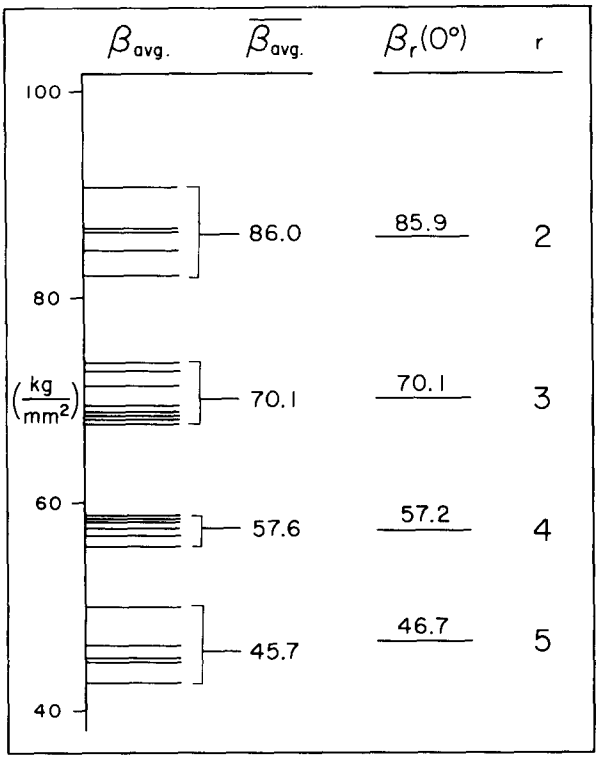

FIG. 2. Comparison of averaged experimental coefficients with those given by Bell's generalized parabolic stress–strain relationship.

the thermomechanical histories of the specimens; that is, it was not possible to consider all impact specimens identical. Furthermore, residual strain measurements along the hitters and specimens indicated occasional inconsistencies with respect to magnitude and symmetry. If an impact test employs a hitter and specimen which have the identical stress–strain relationship and the rod lengths are the same, then the residual strain distributions should be identical. An example of such a test is seen in Fig. 3, test 1028. Only when such coalescence exists can maximum strains be simply calculated from the particle velocity relationship of equation (4) by associating the maximum strain with an impact velocity which is half the hitter velocity. Fig. 3 also shows for test 1200 a large difference in residual deformation. This resulted from employing a hitter possessing no atypical history from the annealed state and a specimen which was previously plastically impacted but here turned around so as to subject the undeformed end to impact. This means that prior to impact at least the first 15 cm of the specimen differed undetectably from the hitter and the maximum strains would be expected to be the same. The residual non-symmetry indicates that the previously elastically stressed specimen possessed a higher deformation mode (lower value of r) than the hitter. Test 1201 employed a similar specimen and yielded $r = 0$.

The four groups of Fig. 2 cannot be attributed to experimental scatter. This possibility should be considered in view of the data of Dillon [10] for small amplitude plastic waves in annealed aluminum. He concluded that "the dynamic response of annealed aluminum in the plastic range is such that there is a real, large variation in the propagation speed"

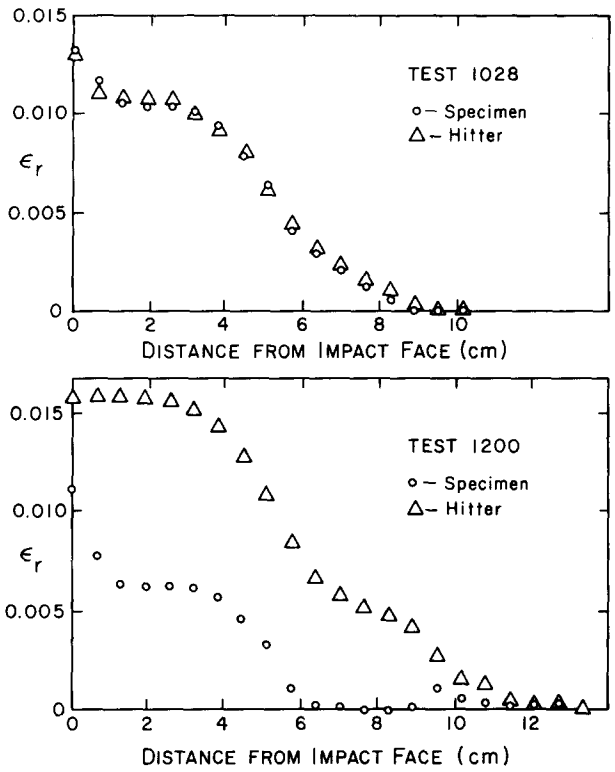

FIG. 3. Residual radial strain distributions for symmetrical (1028) and asymmetrical (1200) impacts.

for strains near yielding. These strains ranged up to about twice the yield strain. The same scatter existed in the present experiments, but is not here studied. In fact, that is why the strain values in Table 2 begin at 0·003 instead of 0·0025, which is roughly twice the average dynamic yield strain, 0·0011.

In [10] it was also concluded that the speeds of propagation of strain levels, which were at least three times greater than the yield strain, were constant and the scatter decreased with increasing strain. The author thus concluded that for *large* amplitude plastic waves the material was adequately described by the strain–rate independent theory. However, he considers "large" strains which are small in comparison with those measured by Bell [1]; and the scatter is still large when compared to the results of Gillich [11] for impacts identical to those studied by Bell. As in [10], Gillich used wire resistance strain gages and found that in 42 tests, employing gages from $\frac{1}{2}$ to $3\frac{1}{2}$ in., the measured response was *inaccurate* when compared to the superior diffraction grating measurement of strain. On the other hand, Gillich's measurements gave consistently more precise results for strains ranging from 0·005 to 0·02 than those in [10] for strains ranging from 0·0005 to 0·0014: the average deviation in [11] is about 5 per cent and in [10] about 13 per cent for data between 2 and 4 in. Thus the conclusion in [10] that the variation in test data decreases with increasing strain is strengthened. The relevant point regarding the present investigation is that the strain levels studied are *large*, up to 25 times the yield strain, and therefore scatter of the type portrayed in [10] is not anticipated.

For the data considered here, uncertainties in measured values can be reasonably estimated and therefore expected deviations may be calculated. For example, for a mode index $r = 3$ and estimated uncertainties of $\Delta t = 10^{-6}$ sec, $\Delta\varepsilon = 0{\cdot}0005$ and $\Delta X = 0{\cdot}30$ mm, the expected deviations for the parabola coefficient are $\Delta\beta = 9$ per cent for $\varepsilon = 0{\cdot}005$ and $\Delta\beta = 6$ per cent for $\varepsilon = 0{\cdot}01$. The values in Table 2 for the tests included in the group $r = 3$ yield average deviations of 5 and 8 per cent respectively. Thus the scatter within a group corresponds closely to that expected from the estimated uncertainties. Therefore, it is maintained that the four deformation modes are real. Although the value of the mode index cannot be predicted *a priori*, there exist certain abnormalities which may be correlated with some of the values of r. A brief discussion of these follows.

Specific atypical histories existed for at least two tests for each of the groups $r = 2, 4, 5$. Two tests yielding $r = 2$ employed hitters and specimens which following annealing were placed in vise grips and subjected to appreciable vibrations caused by the removal of 3 in. of the rod by sawing. The strain–time data for one of these is shown in Fig. 4, wherein

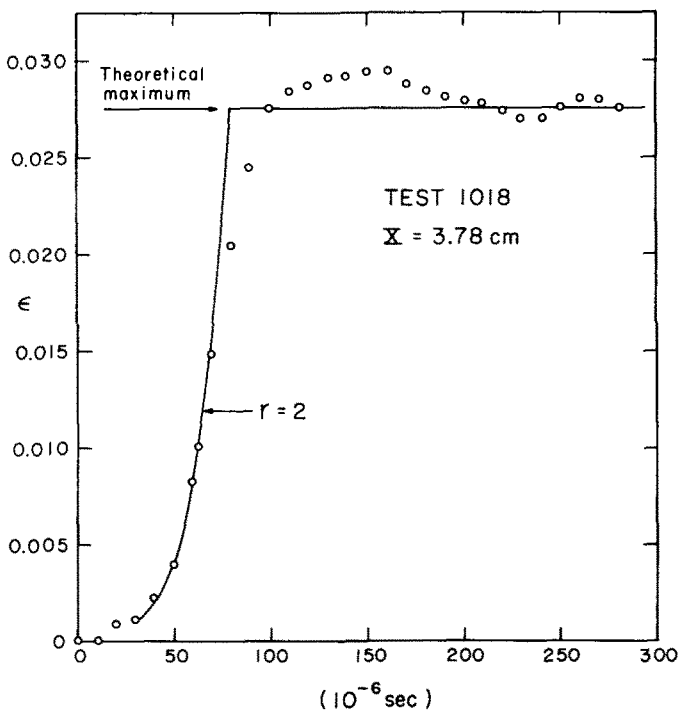

FIG. 4. Strain–time curve for a symmetrical impact governed by the mode index $r = 2$.

the maximum is seen to agree with that predicted. A specimen which was annealed after machining also gave $r = 2$ propagation data. Two specimens which had been subjected to elastic impacts yielded $r = 4$ in plastic impacts. A specimen which was annealed twice and two others subjected to unusually slow cooling from the anneal gave $r = 5$ parabolas. these facts do not conclusively indicate mode correspondence with particular histories; nevertheless, an important observation is that no such history existed for any of the tests

yielding $r = 3$, which is the deformation mode index occurring most often. This is the mode index found by this author [2] to predominate in quasi-static dead-loading tensile deformations of annealed high-leaded brass polycrystals. Also in that investigation, employing the aggregate theory, the same deformation mode was found to describe single crystalline stage III tensile deformations of various α-brass compositions.

It is worthwhile to give some more examples of how well the discrete modes fit the data. Test 1133, shown in Fig. 5, depicts the agreement with the parabolic law for a symmetrical

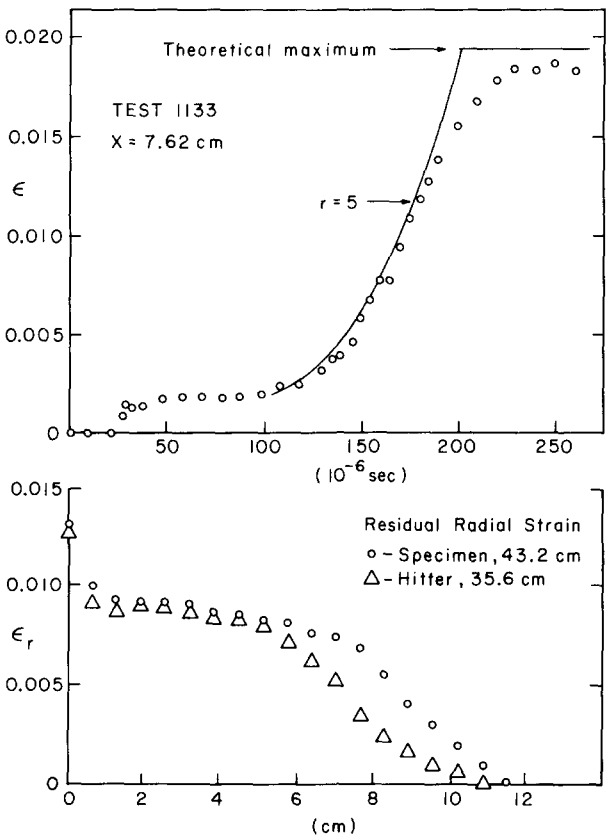

FIG. 5. Parabola agreement with strain arrival outside the maximum strain region.

impact. The grating was located outside of the maximum strain region and therefore the theoretical maximum strain has been reduced in proportion to the ratio of the residual strains at the grating location and the plateau region. Also, since in this test the hitter is shorter than the specimen, it becomes unloaded sooner, as evidenced by the residual strain distributions. The first diameter delay effect is illustrated in Fig. 6, which shows two symmetrical tests for which the gun pressures were the same and the gratings were 1·90 cm apart. The propagation times from the $r = 3$ parabola for the indicated values of strain to travel this distance predicts the strain–time curve at the downstream position (1046) from that upstream (1024); thus demonstrating that the delay in arrival from the origin

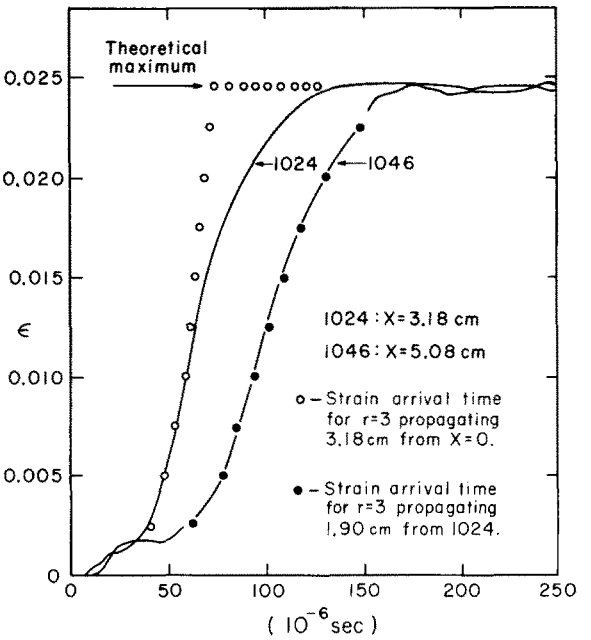

FIG. 6. Two symmetrical tests for $r = 3$, showing identical upper strain delays from the origin.

is the same for each and that the wave speeds are constant, scaling as X/t. Similar visualizations of this agreement with equation (3) could be presented for each of the other groups; but that is already implied, at least for strains up to the surface angle maximum, in the interpretation of Fig. 2.

The essential result of the data analysis is the agreement with the discrete values of equation (2). Furthermore, having established the operative value of r from the arrival times, the maximum strain is then found to be that predictable from the known impact speed. The data is well described by the generalized stress–strain relation and the introduction of $\dot{\varepsilon}$ into the response function is not necessary. This does not mean that strain–rate effects do not exist. The behavior near the yield point is similar to that reported in [10] and may well be best described by a viscous model. However, the order established for the *large* amplitude plastic wave was accomplished through use of the strain–rate independent theory.

Large elastic stress anomaly

While the constitutive assumption, $\sigma = \beta\varepsilon^{\frac{1}{2}}$ provides excellent agreement with wave speeds and maximum strains, there exists anomalous stress behaviors. Since the impact problem has been formulated and observed in terms of strain, it has not been necessary to discuss stress in order to obtain the above agreement with the generalized parabolic law. The degree of the unloading phenomenon, the large elastic step on most of the strain–time curves and the appreciable static yield stress, all indicate the existence of a large elastic stress wave in the impact experiments. Impact tests wherein the specimen was backed up by a long hard bar showed the elastic wave to have a magnitude of about 13 kg/mm^2. This suggests inconsistency with the assumed stress–strain relation for none of the parabolas

yield even maximum stresses this large. Furthermore, this same anomaly has been found to exist for other materials. Magnesium and zinc were found in impact studies to be governed by parabolas with respect to wave speeds and maximum strains even though appreciable yield stresses existed which propagated elastically.

An explanation for this apparent discrepancy is that while for impact velocities below the yield velocity the wave initiation is simple and requires elastic considerations only, exceeding the yield velocity results in an entirely different wave formation in the first diameter. The existence at the impact face of peak stresses has been documented in [6] and [12]. It is probable that the plastic wave formation is determined wholly from the parabolic constitutive equation independent of the existing peak stress, whose collapse at the impact face results in a two wave structure; one of which propagates elastically with the magnitude of the yield stress; the other being the plastic wave with its associated first diameter behavior. Since the balance of stress and velocity across the impact face are trivially satisfied for symmetrical impacts, it is of interest to consider the maximum strain prediction when the hitter is hard; for then the stresses and velocities across the impact

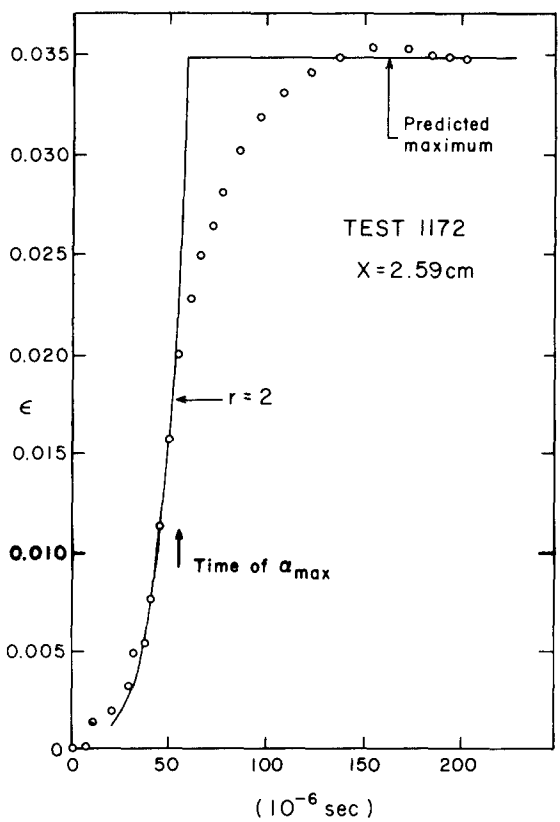

FIG. 7. Parabola agreement in test employing a hard hitter.

face are not trivially balanced. In Fig. 7 the predicted maximum was obtained by balancing the elastic stress and the velocity of the hard bar with the stress and particle velocity given

by the $r = 2$ parabola. The resulting equation is:

$$V_H - \frac{\beta(\varepsilon_{max})^{\frac{1}{2}}}{(\rho_0 C_0)_H} = \frac{4}{3}\frac{(\beta/2\rho_0)^{\frac{1}{2}}}{(\varepsilon_{max})^{-\frac{1}{4}}}, \tag{8}$$

where c_0 is the elastic wave speed. The excellent agreement supports the contention that the parabolic law alone governs the wave formation at the impact face.

Compressibility anomaly

As a result of carefully checking the residual deformation distribution in these experiments, a previously unreported phenomenon has been observed. This concerns the long time "post wave" growth of the residual radial strains. Comparing radial strain measurements, which were performed one year after impact, with those made the day of the test a marked difference is noticed. An example is shown in Fig. 8. It is seen that not only has the maximum increased but also the deformation has penetrated further down the rod.

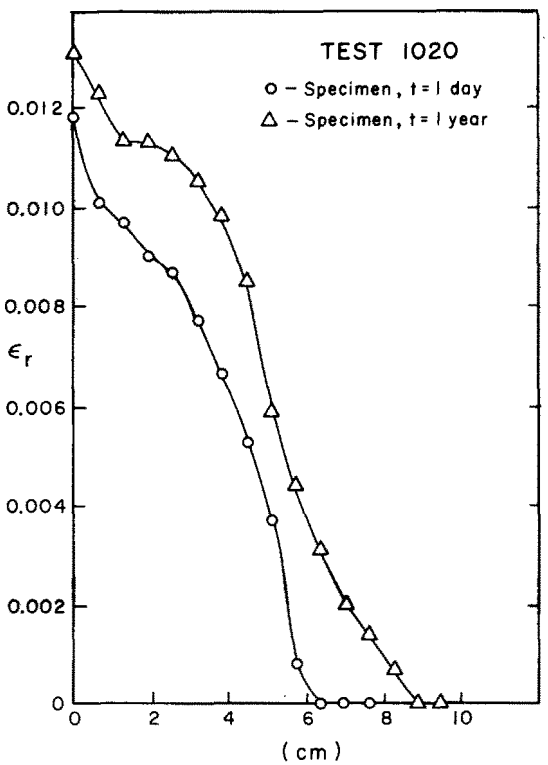

FIG. 8. Radial strain distributions in impacted rod showing "post wave" growth.

The initially measured radial strains are usually too low for agreement with the maximum longitudinal strains as measured by the diffraction gratings if incompressible macrodeformation is assumed. However, although the maximum radial strain may increase to as great as 1·5 times its initial value in a year, the longitudinal strain apparently remains unchanged. If the deformations, especially the "post wave" kind, were isochoric, then the

longitudinal strains would change nearly twice the amount of any radial change. In particular, test 1020 (Fig. 8) exhibits a swelling away from the impacted configuration, and if this involves no volume change, then longitudinally the rod should have recovered 0·006 strain at the diffraction grating location, 3·68 cm. Microscopic measurements of the grating width indicated that the longitudinal strain had remained at that value which was measured dynamically; namely, 0·020. Thus, after sufficient time, the longitudinal strain measured on the surface and the radial strain are compatible for an incompressible deformation from the initial ($t = 0$) configuration.

The tendency of the volume of the deformed configuration towards the volume of the undeformed configuration is characteristic of all specimens which exhibit a change in residual radial strain. This growth did not occur in all impacted annealed rods; however, sufficient time for noticeable change varies from test to test. Whereas one rod may change appreciably in a year, another shows little change in that time but additional growth later. There is evidence that the manner of unloading can strongly affect the development of this growth; and mild indications of distinctive long time behaviors for different deformation phases have been observed.

The basic characteristics of this phenomenon; namely, dilatational variance, implies disharmony with the generally accepted idea that plasticity of metals is an isochoric deformation. However, quasi-static deformations of brass, which are discussed in [2], were incompressible and no change in the residual radial strains were observed. Also, for slow deformations of annealed copper and aluminum rods, simultaneous measurements of axial and radial strains indicated instantaneous incompressibility up to 2 per cent axial strain.* An important distinction here is that the unusual behavior follows dynamic impacts of annealed rods, whose one dimensional description has been seen to include other heretofore unnoticed subtleties. Preliminary investigations indicate that this phenomenon occurs infrequently in aluminum to a much less degree than in brass.

Since a systematic study of this effect requires periodic observations for several years, additional discussion can not be given now.

CONCLUSIONS

It has been shown that the impact response of annealed polycrystalline α-brass is expressible in terms of the discrete deformation modes of the generalized parabolic stress–strain relationship. The applicability of that relationship illustrates that the dynamic deformation of this low stacking-fault energy, face-centered cubic solid can be described by the finite amplitude wave theory to the same quantitative degree as that of the high stacking-fault energy metal, aluminum. Thus, the inclusion of "strain rate" into the constitutive equation is unnecessary.

One aspect of the dynamic deformation for which brass differs from aluminum concerns an uncertainty in predicting the deformation mode. The mode which will be operative in an impact test is dependent on material history. Within the bounds of mild history variations, which yield no change in the dynamic deformation mode of aluminum, several modes occurred for brass. However, a particular deformation mode, occurring for no atypical history, predominates not only for the dynamic tests but also for quasi-static deformations of both polycrystals and single crystals, as shown previously by this author [2]. Thus, for

* Private Communication with T. S. Dawson at the Johns Hopkins University.

three distinct deformation studies, employing several purities of this substitutional solid solution and covering a range of strain rates from "zero" to 10^4 sec^{-1}, a constant description is afforded by the use of the generalized constitutive equation of Bell [1].

Acknowledgments—The author is grateful for many discussions with Professor James F. Bell, especially for his encouragement during the course of the research. The technical assistance of Mrs. Faith Paquet and Mr. John Gottschalk is sincerely appreciated. Portions of this work were sponsored by the United States Air Force Office of Scientific Research and the United States Army Ballistic Research Laboratories.

REFERENCES

[1] J. F. BELL, *The Physics of Large Deformation of Crystalline Solids.* Springer Tracts in Natural Philosophy, 14 (1968).
[2] W. F. HARTMAN, The applicability of the generalized parabolic deformation law to a binary alloy. Ph.D. thesis, The Johns Hopkins University (1967).
[3] J. F. BELL, Normal incidence in the determination of large strain through the use of diffraction gratings. *Proc. 3rd U.S. Nàtn. Congr. appl. Mech.* 489 (1958).
[4] T. VON KARMAN, On the propagation of plastic deformation in solids. *National Defense Res. Council*, Rept. A-29 (1942).
[5] G. I. TAYLOR, The plastic wave in a wire extended by an impact load. *British Ministry of Home Security Civil Defense*, Res. Committee, Rept. R.C. 329 (1942).
[6] G. L. FILBEY, Intense plastic waves. Ph.D.Dissertation, The Johns Hopkins University (1961).
[7] J. F. BELL and W. M. WERNER, Applicability of the Taylor theory of the aggregate to finite amplitude wave propagation in copper. *J. appl. Phys.* **33**, 2416 (1962).
[8] J. F. BELL, Study of initial conditions in constant velocity impact. *J. appl. Phys.* **31**, 2188 (1960).
[9] W. J. GILLICH, Propagation of finite amplitude waves in single crystals of high-purity aluminum. *Phil. Mag.* **15**, 659 (1967).
[10] O. W. DILLION, JR., Experimental data on small-plastic deformation waves in annealed aluminum. *Int. J. Solids Struct.* **4**, 197 (1968).
[11] W. J. GILLICH, The response of bonded wire resistance strain gauges to large amplitude waves in annealed aluminum. Essay, The Johns Hopkins University (1960).
[12] J. F. BELL and J. H. SUCKLING, The dynamic overstress and the hydrodynamic transition velocity in the symmetrical free flight plastic impact of annealed aluminum. *Proc. 4th U.S. Natn. Congr. appl. Mech.* 877 (1962).

(*Received* 19 *April* 1968; *revised* 16 *September* 1968)

Абстракт—Экспериментальное исследование распространения волны большой амплитуды в отожженных поликристаллах α-латуни указывает на применимость обобщенной параболической зависимости напряжение-деформация к двойному сплаву с низкой энергией дефекта упаковки. Находятся, что отдельные формы дискретных деформаций действительно зависят от истории материала прежде свободного удара стержней.

Константируется, что результаты согласные с квази-статической деформацией отдельных кристаллов и поликристаллов латуни. Дается вывод, что несмотря на большую разницу в энергиях дефекта упаковки латуни и алюминия, деформации каждого металла можно точно описать без подробного включения "скорости деформации" в определяющее уравнение.